Mechanism of Base-Promoted Dehydrochlorination of Pentachloroethane: Concerted or Stepwise?

Xiandong Liu*,†,‡ and Evert Jan Meijer*,‡

State Key Laboratory for Mineral Deposit Research, School of Earth Sciences and Engineering, Nanjing University, Nanjing 210093, People's Republic of China, and Van't Hoff Institute for Molecular Sciences and Amsterdam Center for Multiscale Modeling, University of Amsterdam, Nieuwe Achtergracht 166, 1018 WV Amsterdam, The Netherlands

Received: February 2, 2009; Revised Manuscript Received: February 26, 2009

This paper reports a first-principles molecular dynamics simulation study of the microscopic mechanism of the base-catalyzed dehydrochlorination of pentachloroethane. So far the nature of the mechanism of this reaction is not understood: the concerted and stepwise mechanisms are under debate. By combining ab initio molecular dynamics with the method of constraints, we determine the reaction mechanism and associated free energy profile. We find that the reaction barrier is in good agreement with experimental findings and reveal that the reaction proceeds via a concerted mechanism. Our simulations provide no evidence for the presence of carbanion intermediate indicative of the stepwise pathway. This microscopic understanding will provide new implications for understanding the reduction of polyhalogenated alkanes and rational design of effective materials to treat these contaminants.

1. Introduction

Dehydrochlorination of pentachloroethane (PCA) is a typical base-promoted reaction

$$CHCl_2CCl_3 + OH^- \rightleftharpoons CCl_2CCl_2 + HOH + Cl^-$$

The detailed reaction mechanism is important for understanding structure−reactivity relationships and reduction of polyhalogenated alkanes.[1,2] For this reaction, there are two possible pathways: the concerted (E_2) and the stepwise (E_{1CB}). The E_2 pathway means that the elimination of H^+ and Cl^- happens at the same time, whereas in E_{1CB} there is the initial formation of a carbanion intermediate ($[CCl_3CCl_2]^-$), which then degrades to CCl_2CCl_2 and Cl^-. These two mechanisms are experimentally indistinguishable. So, although many experiments have been conducted, the real mechanism is still unclear.[1,2]

Recent interest in this reaction mechanism originates from design of effective environmentally friendly materials to treat polyhalogenated alkanes.[3,4] For example, it has been demonstrated that the reduced iron-bearing smectites can significantly promote PCA degradation and therefore they can play important roles in controlling these species.[3] Generally, it is believed that reduction of structural iron in smectites increases the surface electronic density and this makes interface water molecules more basic, which thus accelerate PCA dehydrochlorination. But the atomistic level mechanism is still open. Besides the PCA reaction step, this surface-catalyzed process also includes some diffusion steps, e.g., adsorption of PCA to smectites and desorption of products, which make the mechanism much more difficult to reveal.[3,4] Obviously, rationalization of the pathway of PCA dehydrochlorination can help clarify the mechanism of this surface reaction.

The aim of this study is to gain insights into the reaction mechanism by using Car−Parrinello molecular dynamics method,[5,6] which has been widely proven effective to study chemical reactions in aqueous solutions. In order to enforce the reaction events, we performed a series of constrained Car−Parrinello molecular dynamics simulations and thus the reaction free energy profile is obtained by integrating the constraint forces. The reaction route is analyzed by investigating the geometries, electronic structures, and hydration structures around the leaving chlorine. These detailed analyses suggest that the concerted mechanism is more likely rather than the stepwise one.

2. Methods

Molecular dynamics calculations are performed on a system consisting of 32 water molecules, 1 PCA, and 1 hydroxyl in a periodically replicated cubic box of side length 10.5 Å. The electronic structure and the forces on the nuclei of the atoms in the system are calculated in the framework of density functional theory. The exchange-correlation is described by BLYP functional, which adopts the local density approximation augmented with the generalized gradient approximation for the exchange part proposed by Becke[7] and for the correlation part by Lee, Yang, and Parr.[8] It has been proven that BLYP can accurately describe the behaviors of water and proton, e.g.[9−11] The norm-conserving Martins−Trouillier pseudopotentials[12] are used to describe the interaction of the valence electrons and the core states, and the Kleinman−Bylander scheme[13] is applied. The orbitals are expanded in a plane wave basis set with a kinetic energy cutoff of up to 70 Ry.

The molecular dynamics simulations are performed using the Car−Parrinello approach as implemented in the CPMD package (CPMD version 3.11).[6] If hydrogen is assigned the mass of deuterium, the equation of motion is integrated with a time step of 0.168 fs and the fictitious electronic mass is set to 1000 au, which maintain the adiabatic conditions. As the reaction rate is beyond the time scale of the regular CPMD simulation, the

* Corresponding authors, xiandongliu@gmail.com and e.j.meijer@uva.nl.
† Nanjing University.
‡ University of Amsterdam.

10.1021/jp900944g CCC: $40.75
Published on Web 03/23/2009

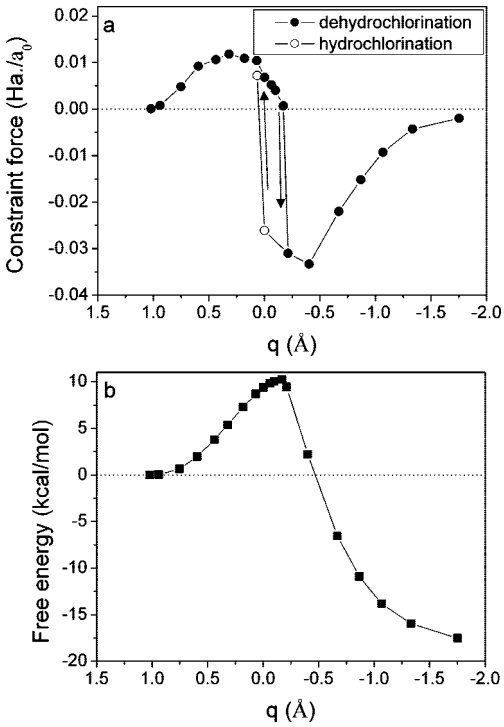

Figure 1. (a) The calculated constraint force curve. The arrows indicate the reaction directions. (b) The free energy profile. The first point of the dehydrochlorination route (q = 1.1 Å) is taken as the reference of the free energy profile.

reaction event is enforced with the method of constraints.[14,15] The difference between the $O_{OH}-H_{PCA}$ distance and $H_{PCA}-C_{PCA}$ distance is taken as the reaction coordinate (q). For a series of values of the reaction coordinate, a molecular dynamics simulation is performed, each of which lasts 6−10 ps. The temperature is set at 300 K and imposed with the Nosé-Hoover thermostat. The free energy profile is calculated by integrating a fit through the average constraint force values. The reverse hydrochlorination reaction is also simulated. The statistics are collected every four steps for all simulations.

3. Results and Discussion

Figure 1 shows the calculated constraint force curve and associated free-energy profile. For the dehydrochlorination reaction, we see that up to q = −0.16 Å the constraint forces are positive and the free energy increases; inspection of the trajectories shows that in this part of the reaction a PCA−OH^- complex has formed (Figure 2a). For the simulation at q = −0.16 Å the constraint force is near 0, indicating it is near the transition state region of the reaction pathway (Figure 2b). During the simulation at q = −0.20 Å, the constraint force changes sign and drops substantially. This is a manifestation of a sudden reactive event, namely, the leaving of the chloride anion (Figure 2c, vide infra). Upon further transfer of the proton, the free energy gradually decreases (Figure 2d). The free energy profile shows a barrier of 10.3 kcal/mol in reasonably good agreement with the experimental estimate, 13−15 kcal/mol.[1,2] On the reverse route, we observe a gradual increase of the constraint force upon transfer of the proton from a coordinated water molecule to a carbon of the tetrachloroethene. At the q = 0.064 Å simulation, the constraint force suddenly changes sign and rises significantly to a value just above 0.

Comparing the forward and backward routes, we observe some hysteresis (Figure 1a) which is associated with the sudden

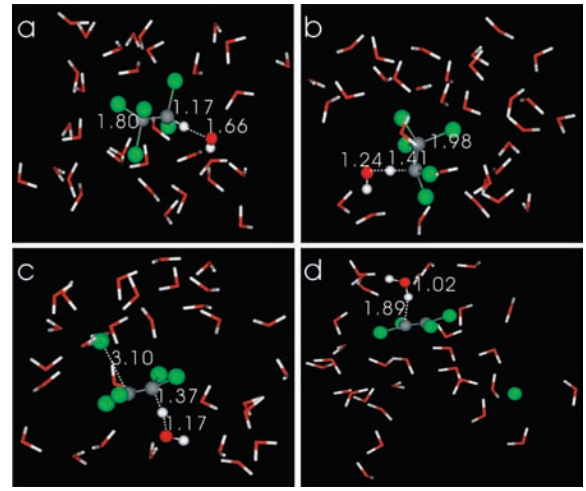

Figure 2. Representative snapshots of PCA dehydrochlorination at the reaction coordinates: (a) q = 0.49 Å, (b) q = −0.16 Å, (c) q = −0.20 Å, and (d) q = −0.87 Å. The molecules participating in the reaction are shown in ball and stick models and the solvent waters are shown as lines. Numbers indicate distances in angstroms. Key: O = red, H = white, Cl = green, and C = gray.

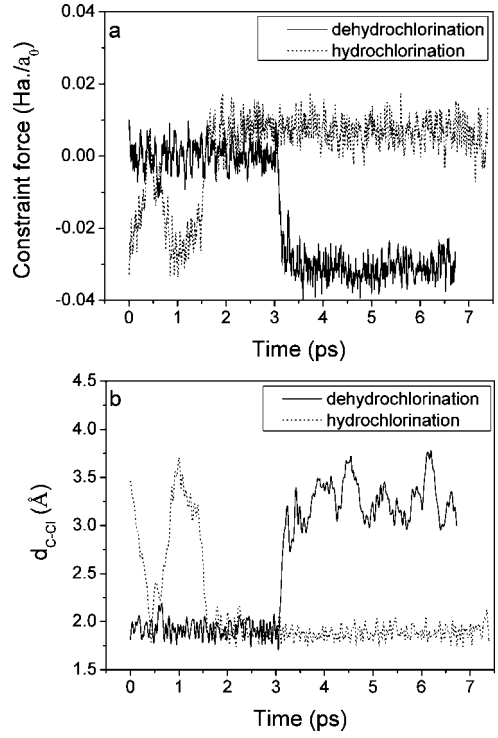

Figure 3. Time evolutions of (a) the constraint forces and (b) C−Cl distances in simulations of dehydrochlorination and hydrochlorination at the reaction coordinates of q = −0.20 Å (solid) and q = 0.064 Å (dash), respectively.

change observed in both routes. It indicates that the imposed reaction coordinate does not capture all of the structural rearrangements associated with this reaction. The value of the proton transfer coordinate at the true transition state (q^{TST}) is expected to be in between the zero-constraint values of the forward and backward route, 0.064 Å > q^{TST} > −0.20 Å.

Figure 3 shows the time evolutions of the constraint forces and C−Cl (the leaving chloride and the bonded carbon) distances for the simulations that show sudden sign reversal of constraint forces in the forward (q = −0.20) and backward (q = +0.064) routes. For the dehydrochlorination reaction (q = −0.20; solid line in Figure 3a), the constraint force fluctuates

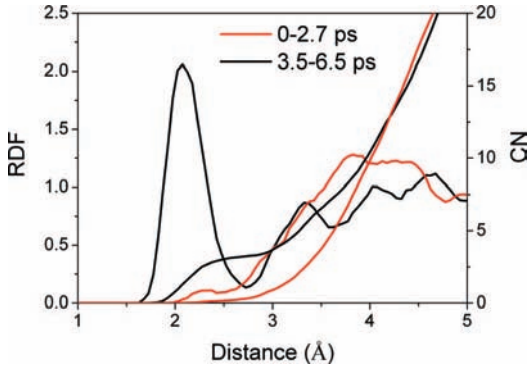

Figure 4. Radial distribution functions (RDF) and coordination numbers (CN) for water H around the leaving Cl before and after reaction happens during the dehydrochlorination simulation at the reaction coordinate of $q = -0.20$ Å.

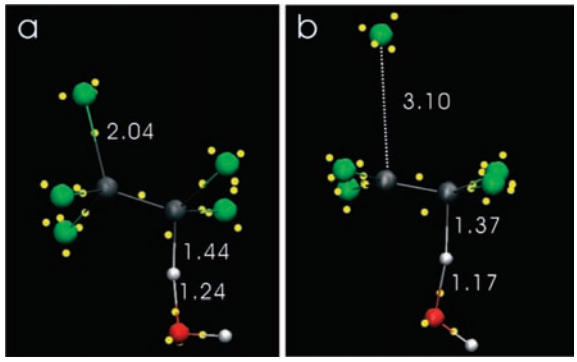

Figure 5. Wannier function centers in dehydrochlorination simulation at the reaction coordinate $q = -0.20$ Å, derived at (a) 2.5 ps and (b) 3.7 ps.

around 0 during the first 3.1 ps, which indicates that those configurations are located near the transition state region. During that period, the C−Cl distances are around 1.90 Å (solid line on Figure 3b), which is the typical bond length in PCA. At about 3.1 ps, the constraint force decreases significantly together with a substantial increase of the C−Cl distance, indicating bond breaking. For simulation of the hydrochlorination reaction ($q = +0.064$), the sudden sign reversal of the constraint force happens at about 1.8 ps (dashed line on Figure 3a) and is accompanied by a significant decrease of the C−Cl distance to a typical bonding value of 1.90 Å (dashed line in Figure 3b).

After the dehydrochlorination reaction happens, the solvation structure of the leaving chlorine changes rapidly. Figure 4 shows the radial distribution functions (RDF) and coordination numbers (CN) for Cl−H before and after detachment of chlorine. No clear peaks are identified on the RDF before reaction, which indicates that there is no direct correlation between Cl and the surrounding water molecules. Integration of this RDF up to 2.5 Å yields a coordination number of about 0.02, which indicates that water molecules only occasionally get close to the leaving chlorine. On the RDF after reaction, the well-defined first peak ranges from 1.7 to 2.7 Å, which corresponds to the first hydration shell of chloride in aqueous solutions.[16] Therefore, to arrive at a smooth and reversible pathway the process of C−Cl bond breaking formation should also be controlled by incorporating, e.g., the C−Cl bond length or the water coordination of the chloride anion in the imposed reaction coordinate.

Detailed insight into the change of electronic structures during the reaction is provided by Wannier function centers (WFCs),[17] which provide important chemical insight as they can be associated with a bonding or lone pair of electrons. Figure 5 shows the WFCs derived with the configurations before and after dehydrochlorination occurs. Compared with Figure 5a, it is clear that after dehydrochlorination, the proton has transferred to the hydroxyl, Cl^- goes off, and simultaneously a C−C double bond has formed.

4. Conclusion

In conclusion, our simulations of the dehydrochlorination reaction of PCA do not show the presence of carbanion intermediate indicative of the stepwise E_{1cb} mechanism. In contrast we observe that the dehydrochlorination occurs via a concerted E_2 pathway: the process of chloride−carbon bond breaking and associated chloride solvation requires the leaving proton to be nearly halfway to its transfer to a water molecule ($0.064 > q^{TST} > -0.20$). Improving the sampling of the reaction pathway by controlling explicitly the chloride−carbon bond distance and/or the chloride solvation would yield a better and more reversible description of the reaction pathways but would not change the nature of the reaction mechanism. In future study, the dehydrochlorination reaction promoted by the reduced Fe-containing smectites will be addressed.[3,4] In that case, the surface waters act as a Brønsted base, which actually catalyzes the dehydrochlorination. Understanding these reactions in atomistic detail is important for design of environmentally friendly materials.

Acknowledgment. We acknowledge the Jiangsu Project Innovation for Ph.D. Candidates (CX07B-049z) and the Scientific Research Foundation of the Graduate School of Nanjing University.

References and Notes

(1) Roberts, A. L.; Gschwend, P. M. *Environ. Sci. Technol.* **1991**, *25*, 76–86.
(2) Walraevens, R.; Trouillet, P.; Devos, A *Int. J. Chem. Kinet.* **1974**, *41*, 777–786.
(3) Cervini-Silva, J.; Wu, J.; Stucki, J. W.; Larson, R. A. *Clays Clay Miner.* **2000**, *48*, 132–138.
(4) Cervini-Silva, J.; Larson, R. A.; Stucki, J. W. *Langmuir* **2006**, *22*, 2961–2965.
(5) Car, R.; Parrinello, M. *Phys. Rev. Lett.* **1985**, *55*, 2471.
(6) CPMD, Copyright IBM Corp 1990−2006, Copyright MPI für Festkörperforschung Stuttgart 1997−2001. The CPMD-3.11.1 version was used.
(7) Becke, A. D. *Phys. Rev. A* **1988**, *38*, 3098–3100.
(8) Lee, C.; Yang, W.; Parr, R. G. *Phys. Rev. B* **1988**, *37*, 785–789.
(9) Laasonen, K.; Sprik, M.; Parrinello, M.; Car, R. *J. Chem. Phys.* **1993**, *99*, 9080–9089.
(10) van Erp, T. S.; Meijer, E. J. *Angew. Chem., Int. Ed.* **2004**, *43*, 1659–1662.
(11) Marx, D.; Tuckerman, M. E.; Hutter, J.; Parrinello, M. *Nature* **1999**, *397*, 601–604.
(12) Troullier, N.; Martins, J. L. *Phys. Rev. B* **1991**, *43*, 1993.
(13) Kleinman, L.; Bylander, D. M. *Phys. Rev. Lett.* **1982**, *48*, 1425.
(14) Curioni, A.; Sprik, M.; Andreoni, W.; Schiffer, H.; Hutter, J.; Parrinello, M. *J. Am. Chem. Soc.* **1997**, *119*, 7218–7229.
(15) Sprik, M.; Ciccotti, G. *J. Chem. Phys.* **1998**, *109*, 7737–7744.
(16) Heuft, J. M.; Meijer, E. J. *J. Chem. Phys.* **2003**, *119*, 11788–11791.
(17) Silvestrelli, P. L.; Marzari, N.; Vanderbilt, D.; Parrinello, M. *Solid State Commun.* **1998**, *107*, 7–11.

JP900944G